applied sciences

MDPI

Article

Industrial Robot Positioning Performance Measured on Inclined and Parallel Planes by Double Ballbar

Ivan Kuric [1], Vladimír Tlach [1,*], Milan Sága [2], Miroslav Císar [1] and Ivan Zajačko [1]

[1] Department of Automation and Production Systems, Faculty of Mechanical Engineering, University of Zilina, 010 26 Zilina, Slovakia; ivan.kuric@fstroj.uniza.sk (I.K.); miroslav.cisar@fstroj.uniza.sk (M.C.); ivan.zajacko@fstroj.uniza.sk (I.Z.)

[2] Department of Applied Mechanics, Faculty of Mechanical Engineering, University of Zilina, 010 26 Zilina, Slovakia; milan.saga@fstroj.uniza.sk

* Correspondence: vladimir.tlach@fstroj.uniza.sk

Abstract: Renishaw Ballbar QC20–W is primarily intended for diagnostics of CNC machine tools, but it is also used in connection with industrial robots. In the case of standard measurement, when the measuring plane is parallel to the robot base, not all robot joints move. The purpose of the experiments of the present article was to verify the hypothesis of the motion of all the robot joints when the desired circular path is placed on an inclined plane. In the first part of the conducted experiments is established hypothesis is confirmed, through positional analysis on a simulation model of the robot. They are then carried out practical measurements being evaluated the influence of individual robot joints to deform the circular path, shown as a polar graph. As a result, it is found that in the case of the robot used, changing the configuration of the robot arm has the greatest effect on changing the shape of the polar graph.

Keywords: industrial robot; renishaw Ballbar QC20–W; positional analysis; measurement

Citation: Kuric, I.; Tlach, V.; Sága, M.; Císar, M.; Zajačko, I. Industrial Robot Positioning Performance Measured on Inclined and Parallel Planes by Double Ballbar. *Appl. Sci.* **2021**, *11*, 1777. https://doi.org/10.3390/app11041777

Academic Editor: Subhas Mukhopadhyay

Received: 29 January 2021

Accepted: 15 February 2021

Published: 17 February 2021

1. Introduction

The constant increase in automation in industrial areas is also related to the increasing share of industrial robotics applications. According to a press release issued by IFR (International Federation of Robotics), almost two million new robots are expected to be installed in manufacturing plants worldwide between 2020 and 2021 [1]. One of the first steps in creating a robotic application is a selection of a suitable robot according to certain parameters [2]. Key features include workspace size, load capacity, and also the number of controlled axes. Depending on the specific task that will be automated by the industrial robot, the so-called performance criteria are also important.

Performance criteria allow a more detailed look at the robot features. One of the best-known performance criteria of industrial robots is the pose repeatability, which expresses the ability of the robot TCP (Tool Center Point) to repeatedly return to a defined position in the same direction [3,4]. Pose repeatability is also the performance criterion most frequently mentioned in technical data sheets by industrial robot manufacturers [5]. In addition to the performance criterion above, there are many others, all of which are defined in the ISO 9283 standard. This standard defines the individual performance criteria, the method of their calculation, together with the recommended conditions for their measurement [6].

ISO 9283 is further elaborated on in the respective technical report ISO/TR 13309, which aims to provide an overview of metrological methods and measuring equipment for measuring performance criteria [7]. Numerous scientific papers also deal with the issues related to measurement of the performance criteria of industrial robots. In most cases, these measurements are performed using indicators [8–11], laser trackers [12–14], vision systems [15–17], or laser interferometers [18–20] primarily intended for measuring

the properties of CNC machine tools. These measuring devices satisfy the classifications and methods described in the above technical report to varying degrees.

Furthermore, in professional publications, a double ballbar type of a device is experimentally used to measure performance parameters of industrial robots [19,21–23], which, same as the laser interferometers, are primarily intended for evaluating the condition of CNC machine tools [24]. At the Department of Automation and Production Systems, several papers have also been published related to the possibilities of using the given measuring equipment in connection with industrial robots [25–28]. The principle of measurement with the Renishaw Ballbar is based on movement along a circle or an arc with a fixed point of rotation, while a real distance of moving part from the center of the rotation is compared to the ideal one and then the deviations are recorded. Actual measurement utilizes a precise linear encoder [29]. The use of this device in connection with industrial robots is not specified in the standard (ISO 9283) nor in the technical report (ISO/TS 13309) nor in the standard that describes intended usage of such device (ISO 230–4).

The necessity for knowledge of real values of performance criteria is important not only in the creation of a new robotic cell, in connection with the selection of a suitable industrial robot, but also in robotic applications where the industrial robot has been performing a given task already for some time. These are mainly applications that are more demanding on performance criteria, their stability, or predictability of their development thru time. Such tasks are, for example, precision assembly, a dimensional inspection that implements 3D scanners or measuring probes, etc. [25,30]. In such cases, the measurement of performance criteria is necessary to monitor the robot's technical condition or to troubleshoot existing problems. Early detection of changes in the robot's technical condition may prevent a negative impact of these changes on the work process of the robotic application.

The presented paper deals with the measurement of an industrial robot using a double ballbar type of device-Renishaw Ballbar QC20–W. Specifically, its implementation for measurements with a circular motion path located on an inclined plane, resulting in the motion of all six joints of the robot performing a given TCP movement. The measurement conducted in this way provides a significant amount of information about the robot's current technical state, which can be used in connection monitoring or in the troubleshooting process.

2. Motivation

As indicated in the introduction, several measurements with the Renishaw Ballbar QC20–W involving industrial robots were carried out in the past at the Department of Automation and Production Systems, and the results have been published [25–28]. In most cases, these were basic measurements in the XY plane, parallel to the base plane of the WCS (World Coordinate System) and, at the same time, parallel to the robot base. The measurements were done on Fanuc robots, where the WCS is represented by a fixed coordinate system defined by the manufacturer. The same orientation of the measuring plane in the robot's workspace has been chosen by other authors in their papers too [19,21,22]. The said basic type of measurement requires completing two circular paths in the XY plane in a clockwise direction (CW) and two circular paths in the opposite direction (CCW) [31,32]. Figure 1 shows the course of the motion of the individual robot joints (J1 through J6), during the TCP movement in a circular path in the clockwise direction. The graph shows data that was created in the Creo Parametric 5.0.4.0 program using movement simulation of the model of the Fanuc LR Mate 200iC robot, with the simulation conditions given in Table 1.

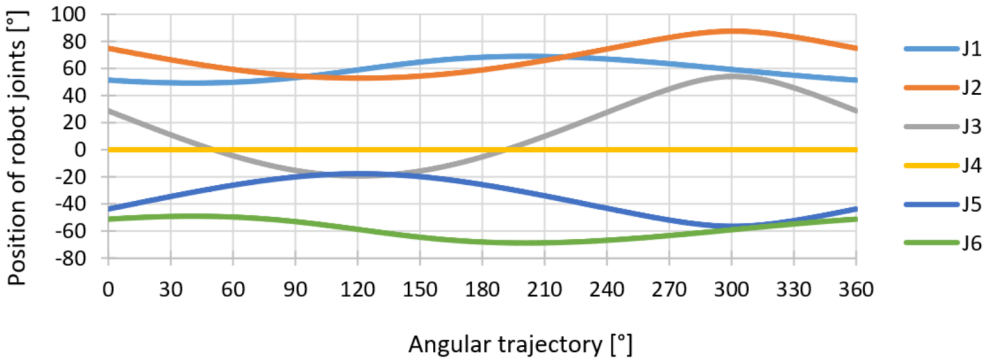

Figure 1. The course of the motion of the individual robot joints during the TCP movement in a circular path in the XY plane.

Table 1. Conditions for creating the circle in the XY plane.

Type of Industrial Robot	Fanuc LR Mate 200iC
The radius of circular paths	100 mm
Centre of circle relative to WCS (X; Y; Z; W; P; R)	300; 500; −253.5; 0; 0; 0
Coordinates of the TCP (X; Y; Z)	0; 0; 74.65

The graph in Figure 1 shows that when the measuring is done in the XY plane, the J4 joint is static for the entire duration of the TCP moving along the circle, therefore, it can be said that the results do not take into account the possible negative effect of the J4 joint motion or that the given results correspond to only one specific position from the range of the J4 joint motion. Regardless of the above statement, the measurement in the XY plane is informative and can be used to evaluate the robot's technical condition. For example, in one of our papers [25], a measurement in the XY plane was used to evaluate the effect of calibration on the accuracy of the resulting movement of the robot's TCP.

In the case of CNC machine tools, to evaluate the effect of movement of all three linear axes (X, Y, and Z), the so-called volumetric analysis, consisting of measurements in three mutually perpendicular planes XY, ZX, and ZY, is used. During the measurement in the XY plane (see Figure 2a) two standard clockwise and two counterclockwise circles are made. In the ZX and ZY planes (see Figure 2b,c) two semicircular paths in the range of 220° are measured, again one in the clockwise and the other in the counterclockwise direction [33,34].

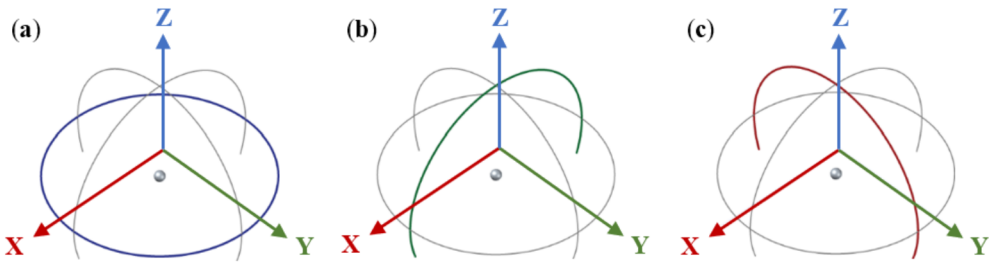

Figure 2. Circular paths in individual planes for volumetric analysis. (**a**) plane XY; (**b**) plane ZX; (**c**) plane ZY.

To verify the possibilities of the volumetric analysis application on industrial robots, a series of measurements were performed in the past on two industrial robots Fanuc LR Mate 200iD and LR Mate 200iD/7L. The circular path and circular arcs with a radius of 100 mm, necessary for measurement purposes, were created through standard programming commands for Fanuc robots. Further information on the measurement conditions is given in Table 2.

Table 2. Measurement conditions for volumetric analysis.

Type of Industrial Robot	Fanuc LR Mate 200iD (E–117096)	Fanuc LR Mate 200iD/7L (E–109256)
The radius of circular paths	100 mm	100 mm
Centre of circle relative to WCS (X; Y; Z; W; P; R)	300; 500; −253.5; 0; 0; 0	300; 500; −253.5; 0; 0; 0
Coordinates of TCP (X; Y; Z)	0; 0; 74.65	0; 0; 74.65
The payload on the end of the robot's arm	438 g	438 g
Speed of TCP	55.33 mm/s	55.33 mm/s
Number of repetitions	30	30
Running-in period before measurement	1 h	1 h

E–117096 and E–109256 represent the serial numbers of the industrial robots used.

The measurements were evaluated in the Ballbar 20 software, with Figures 3 and 4 showing polar graphs of one of thirty repeated measurements for each plane and for both Fanuc robots. In addition to a more detailed analysis of the measurement results, two observations are important for the purposes of this paper.

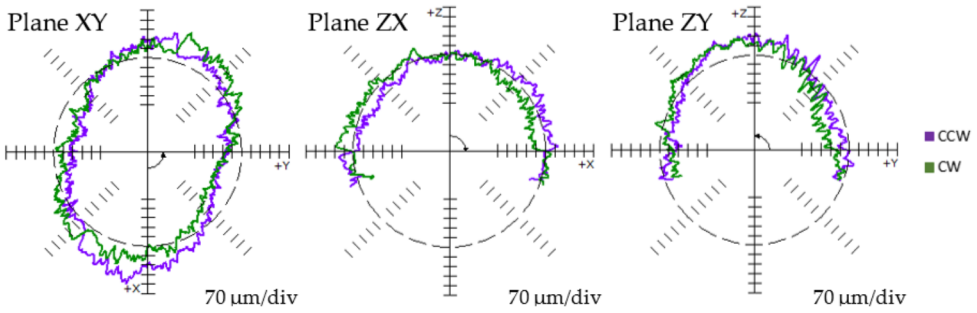

Figure 3. Polar graphs of the volumetric analysis evaluation—LR Mate 200iD.

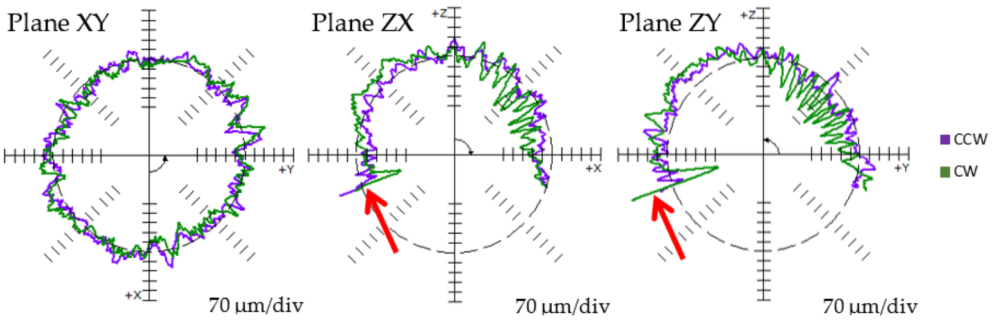

Figure 4. Polar graphs of the volumetric analysis evaluation—LR Mate 200iD/7L.

The first is the "solid line", which is apparent on the polar graphs for the ZX and ZY planes when measured on the LR Mate 200iD/7L robot (Figure 4). This phenomenon occurs due to the continuation of value recording even during the exit at the end of the measurement. As part of the measurement with the Renishaw Ballbar QC20–W, the data recording process is started and ended by entering and exiting the measuring radius. In the case of measuring a circle or a circular arc with a radius of 100 mm, the measurement is started by infeed, a linear movement from the radius of 101 mm to a value of 100 mm, followed by a movement along the circular path itself. On the contrary, after completing a circular path in one direction, the measurement is ended by a feed out, a linear movement to a radius of 101 mm. If the data were also recorded during the feed out from the measuring radius, then this fact is reflected in the already mentioned "continuous line", observed on the polar graph. This phenomenon can be prevented by extending lengths of the infeed and the feed out to more than 1 mm, or by adjusting the speed during these movements. However, in the case of the measurement conducted on the LR Mate 200iD/7L robot, neither of the measures mentioned was effective, and the said phenomenon occurred in all of the thirty repeated measurements. The results of such measurement are skewed

and in order to be used, the data need to be additionally filtered. However, the need for additional filtering results in the necessity for a longer time and more complex processing and evaluation of the measurement. Furthermore, it should be noted that the source of the phenomenon described could also have been the linear sensor used in the measurement. However, in order to refute this claim, further measurements would have to be conducted.

The second of the mentioned observations in the implementation of the volumetric analysis is related to the motion of the industrial robot's individual joints. Figure 5 shows the course of the motion of all six joints of the LR Mate 200iD robot during the TCP movement along a circular path in the ZX plane, within the volumetric analysis. As the graph makes apparent, the J4 joint is static during the entire movement. The situation is the same in the case of the ZY plane. It follows from the above that even in the case of applying the volumetric analysis on an industrial robot, the motion of the J4 joint is not achieved during the measurement.

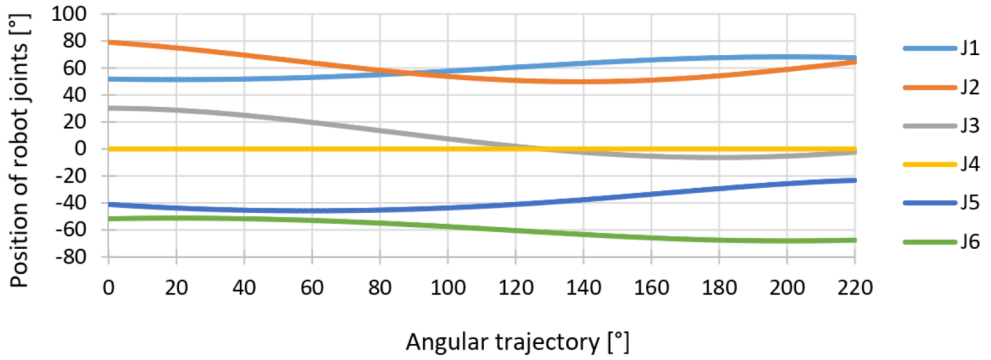

Figure 5. The course of the motion of the individual robot joints during the TCP movement in a circular path in the ZX plane.

In all the presented methods of measurement, whether using a circle or arched paths in the case of the volumetric analysis, the robot's TCP has always moved only in one of some perpendicular planes of the cartesian coordinate system. At the same time, the "Z" axes of the tool coordinate system and world coordinate system were parallel during movement in each of the measuring planes. Therefore, it can be assumed that if both mentioned axes formed a certain angle, the J4 joint would be non-zero and would participate in the given circular motion. One of the possible solutions to achieve the J4 joint motion is to place the desired circle at a certain angle in the robot's workspace. I.e., placing the circle on an inclined plane. With the measurement path designed in this way, it is necessary to verify the correctness of the statement in connection with the J4 joint motion and, at the same time, the possibilities or the ability to conduct measurements with Renishaw Ballbar QC20–W. In the present paper, this hypothesis has been verified, with a positional analysis of the robot's movement in Section 4 by the Creo Parametric 5.0.4.0 system, and inSection 5 by a real measurement done on an industrial robot Fanuc LR Mate 200iC, located in the laboratory of our department.

3. Experiment Preparation

The LR Mate 200iC robot was chosen to conduct the measurement on, with the selection of the position and orientation of the desired circular path in the robot's workspace being the first step. For this purpose, information from the ISO 9283 standard was applied, where the recommended procedure for measuring performance criteria is based on the so-called ISO cube. It is an imaginary cube, its vertices marked C1 to C8, and it is placed in the robot's workspace, with its edges parallel to the robot's basis or its world coordinate system. Based on the industrial robot type, a plane containing points is placed in the said cube, with the points defining the individual paths used for measuring the performance criteria. In the case of robots with six controlled axes, the inclined plane determined by the vertices C1–C2–C7–C8 is selected (see Figure 6) [6]. For the purpose of the experiment, a

circle required for conducting the measurement with the Renishaw Ballbar QC20–W is be placed on this plane.

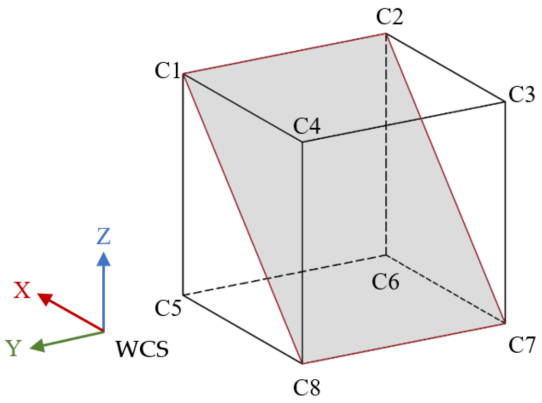

Figure 6. ISO cube with a measuring plane, for robots with six controlled axes.

As for the circle diameter, a basic nominal radius of 100 mm, which had been used in the past experiments, was chosen so that it would be easier to compare the measurement results. Furthermore, it was necessary to determine the position of the ISO cube or the center of the circle in the Fanuc LR Mate 200iC robot's workspace. The base consisted of the coordinates of the center of the circle, used in the present volumetric analysis (see Table 2). However, this position was adjusted so that when the circle was tilted below the angle of $-45°$, the measuring apparatus did not collide with the workbench on which the Fanuc robot was placed. At the same time, the possibilities of the robot arm's reach in the movement along a defined path were also taken into account. As a result, the coordinates of the center of the circle {X = 200; Y = 400; Z = −200} were defined by the Fanuc Roboguide HandlingPRO 8 software.

Two possible configurations of the robot arm correspond to the defined position and orientation of the circle, as well as to the circular path required for the measurement. Specifically, this is a configuration related to the J5 joint position, which is referred to as the N–NOFLIP (joint J5 < 0°) and, as an F–FLIP (joint J5 > 0°) position in Fanuc robots [35]. Both configurations are shown in Figure 7. The measurement was done for each of the two possible configurations of the robot arm.

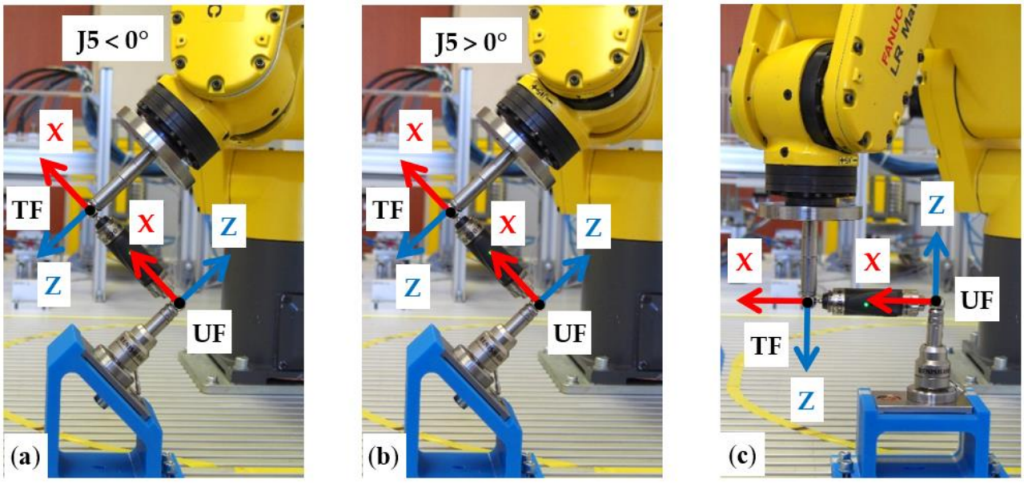

Figure 7. Jigs for measuring in two selected measuring plane. (**a**) NOFLIP configuration; (**b**) FLIP configuration; (**c**) NOFLIP configuration.

To carry out practical measurements, two jigs were designed and manufactured through 3D printing. These allowed the measuring apparatus to be clamped to the robot's

workbench while maintaining the defined coordinates of the center of the circle. The first of the jigs enabled a measurement at an angle of −45° (Figure 7a,b). The second jig was used to conduct a standard measurement in the XY plane parallel to the benchtop (Figure 7c) while maintaining the same coordinates of the center of the circle as was the case with the inclined plane.

The robot's control program was created in such a way that the center of the circle of a given radius was at the beginning of the User Coordinate System (UF) defined concerning the robot's WCS. Through a change in the position or the orientation of the user coordinate system, the program thus created allows a change in the position and orientation of the emergent circle. Thus, the same program is actually used for the desired circle on an inclined plane at an angle of −45° and for the circle in a plane parallel to the benchtop. The programs created in this way are to some extent universal, as they can be used for any position and orientation in the robot's workspace and can also be used on another Fanuc robot. The relative position and orientation of the user (UF) and tool coordinate system (TF) used in the conducted experiments are shown in Figure 7.

4. Positional Analysis in the Creo Parametric System 5.0.4.0

To verify the influence of the selected orientation of the circle on the motion of the robot's individual joints, a positional analysis was created in the Creo Parametric system 5.0.4.0. For the purpose thereof, a simulation model of the LR Mate 200iC robot was created with the kinematic constraints applied. Zero positions of the individual robot joints and their range of motion were defined, corresponding to those of the real robot. The position of the TCP and of the individual coordinate systems was also defined, as was the case with the experiments on a real robot. The simulation conditions are given in Table 3.

Table 3. Simulation conditions for positional analysis.

Type of Industrial Robot	Fanuc LR Mate 200iC
The radius of circular paths	100 mm
Centre of circle relative to WCS (X; Y; Z; W; P; R)	200; 400; −200; 0; −45; 0
Coordinates of the TCP (X; Y; Z)	0; 0; 74.65

The center of the required circular path was located at the zero of the local coordinate system, while its position relative to the WCS robot is shown in Table 3. The circular path itself was created through an inverse kinematics task, by defining the so-called servomotors in the individual axes of motion of the Cartesian coordinate system. The cosine function was used for the direction of the X and Y axes, with its general shape in the Creo Parametric system being the following (1):

$$q = A \cdot \cos\left(360\frac{x}{T} + B\right) + C \quad (1)$$

where the coefficients A = amplitude [mm], B = phase, C = offset [mm] and T [s] represent a period [36]. For the X, Y–axis direction, the required radius of the circle of 100 mm, and the clockwise movement, the given function has the following form (2), (3):

$$q = 100 \cdot \cos\left(360\frac{x}{360}\right) \quad (2)$$

$$q = 100 \cdot \cos\left(360\frac{x}{360} + 90\right) \quad (3)$$

Other axes are defined as constants. Movement in direction of the Z–axis = 0 mm, rotations around the Y and Z axes are also zero (P = 0°; R = 0°). The rotation around the X–axis has a defined value W = −180°, which ensures that the Z–axis of the tool coordinate system has the correct orientation and is perpendicular to the measuring plane or the plane in which the required circle is located.

The results of the positional analysis of the course of motion of individual robot joints are shown in the form of a graph in Figure 8. From the individual trend lines, one can see that all joints of the robot, including the J4 joint, participated in the defined motion. The above graph applies to the clockwise movement of the TCP and to the "NOFLIP" robot arm configuration. For the second configuration ("FLIP"), the graph is similar, with all the joints of the robot participating in the movement. The absolute value of the range of motion of each of the robot's joints is shown in the graph in Figure 9. Because the TCP moved along the same path in both configurations, the displayed range value for both configurations is identical.

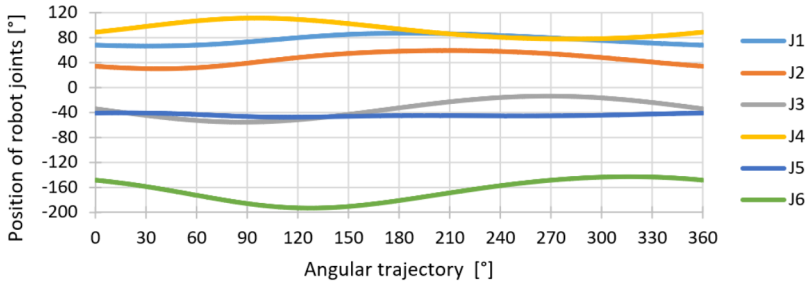

Figure 8. The course of the motion of the individual robot joints during the TCP movement in a circular path in the inclined plane.

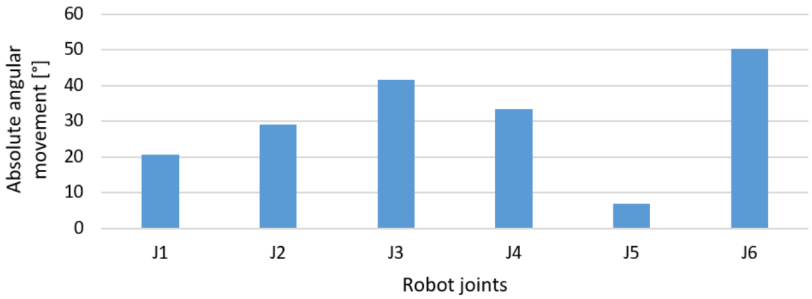

Figure 9. Absolute angular movement of robot joints during the movement along a circular path on the inclined plane.

The present positional analysis confirmed the hypothesis of the robot's individual joints' motion in connection with the location of the required circle on an inclined plane. The next step was to verify the possibilities of practical implementation of such measurement with the Renishaw Ballbar.

5. Measurement with Renishaw Ballbar QC20–W

All the practical measurements presented here were carried on an industrial robot Fanuc LR mate 200iC, located in the laboratory of our department. This robot was examined mainly due to its availability. Basic measurement with the Renishaw Ballbar QC20–W and a circle with a radius of 100 mm placed on an inclined plane (see Figure 6) consisted of two series of measurements with ten repetitions. One series for each of the robot's arm configurations. More detailed measurement conditions are given in Table 4.

The robot control program was created by standard programming commands, such as through connecting two semicircles. For the TCP speed during the measurement, the value of 55.33 mm/s was selected and entered into the robot control program. Such speed corresponds to the federate of 3320 mm/min in the Ballbar 20 software. This speed value is based on experiments conducted in the past [26]. Specifically, it was a comparison of two methods of creating a circular path. The first of the methods was based on the already mentioned connection of two semicircles. For the second method, the circle was created as a polygon, representing the most accurate approximation of the desired circle. The

speed of 55.33 mm/s was then chosen as optimal for the purposes of the said comparison. Subsequently, further experiments with the Renishaw Ballbar were conducted with this speed value, in addition to the volumetric analysis mentioned in the introduction of this paper. At this speed value, the measurement process itself (circle radius 100 mm) with the Renishaw Ballbar takes approximately 53 s. This is a relatively short measurement time, also suitable for the purposes of industrial robot troubleshooting and monitoring.

Table 4. Measurement conditions.

Type of Industrial Robot	Fanuc LR Mate 200iC (E–31806)
The radius of circular paths	100 mm
Centre of circle relative to WCS (X; Y; Z; W; P; R)	300; 500; −253.5; 0; −45; 0
Coordinates of the TCP (X; Y; Z)	0; 0; 74.65
The payload on the end of the robot's arm	438 g
Speed of TCP	55.33 mm/s
Number of repetitions	10 × for configuration N, F, and F′
Running-in period before measurement	1 h

Standard Ballbar 20 software was used to record the measurements, with graphical results in the form of polar graphs shown in Figure 10. By comparing the polar graphs for both robot arm configurations, it is possible to see a significant difference in their shape. The significant difference is also shown in the average value of circularity in Table 5, where the circularity represents the difference between the largest and the smallest radii recorded by the Ballbar during the measurement excluding infeed and feed out. This value is related to the accuracy of the machine in the sense that the higher the circularity value, the worse the accuracy of the machine [37].

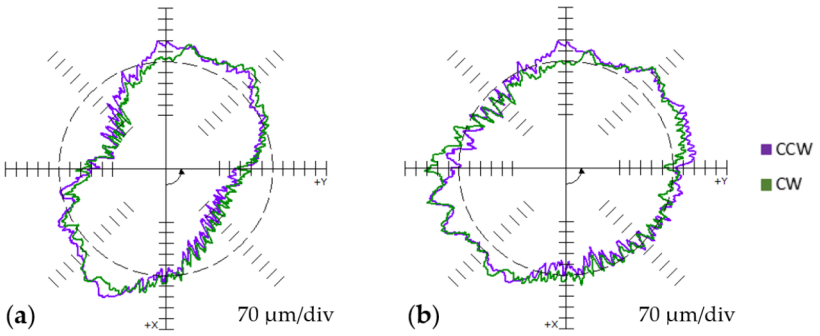

Figure 10. Polar graphs from measuring a circle on the inclined plane. (**a**) NOFLIP configuration; (**b**) FLIP configuration.

Table 5. Average circularity value for both robot arm configurations.

	Configuration NOFLIP	Configuration FLIP
Circularity [µm]	652.2	409.8

The polar graphs mainly show the squareness error and the scaling error. Both of these defects are characterized by the oval shape of the profile or its "peanut" shape. In the case of a squareness error, the axis of such deformation is inclined by 45° or 135°. In the case of CNC machine tools, this error is caused by the fact that the two axes performing the movement are not perpendicular [38]. The second of these errors, the scaling error, is caused by the different magnitude of the movement increment between the axes and is manifested by the said deformation along the axis of movement [38]. Unlike a CNC machine tool, with industrial robots, the circular motion during the measurement is the result of the simultaneous motion of several or all of the robot's joints. For this reason,

these errors can be attributed mainly to the incorrect conversion of Cartesian coordinates, related to the direct kinematic task, and the issue of calibration. Specifically, this is the first level calibration, related to the relationship between the actual position of the robot arm and the information from the encoders in its individual joints [39].

For a more detailed analysis of the measurements, based on the robot's simulation model, a graph was created in Figure 11. This graph shows the range of motion of the robot's individual joints during measurements with both configurations of the robot arm. The graphical representation shows that the movements of the joints J1, J2, and J3 are identical in both configurations. On the contrary, the changes occur only in the orientation of the robot's subsystem, i.e., that of the joints J4, J5, and J6. Based on this analysis, it can be concluded that the change in the shape of the polar graphs (Figure 10) is caused by one of the joints of the robot's orientation subsystem, or a combination thereof.

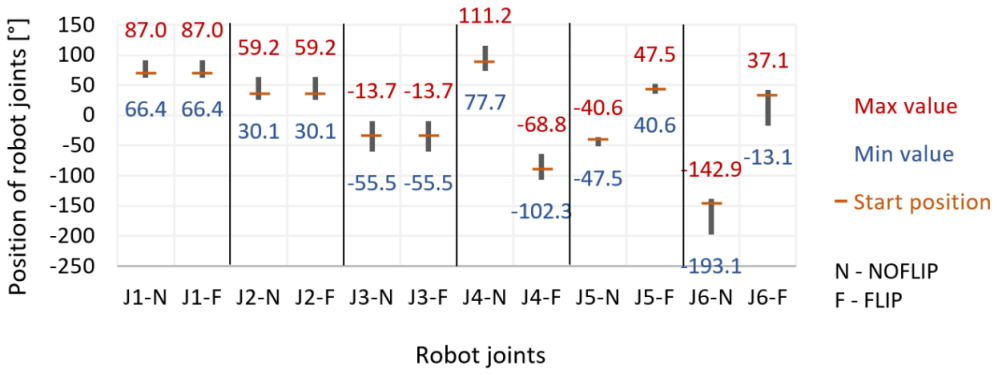

Figure 11. Comparison of the movement of robot joints for both used robot arm configurations.

A more accurate identification of the specific robot joint or joints that adversely affect the measurement results can be addressed in several ways. This involves, for example, limiting the motion of one of the robot's examined joints, or modifying the motion of the joint so that its possible adverse effect is apparent. The graph in Figure 11 shows that the motion of the J6 joint is shifted by 180° relative to each other in both configurations. At the same time, the coordinates of the TCP orientation are constant during the entire circular motion and have the following values (W = 180°; P = 0°; R = 0°). Because the TCP is in the axis of rotation of the J6 joint, the coordinate "R" (rotation around the Z–axis) can influence the way the joint J6 moves.

This theory was first verified in the robot's simulation model. For an arm configuration with J5 > 0° (FLIP), a TCP position was defined with the coordinate R adjusted to 180°. The graph in Figure 12 shows that by applying the said change, the same motion of the J6 joint was achieved as in the NOFLIP configuration. At the same time, there was no change in the J4 and J5 joints.

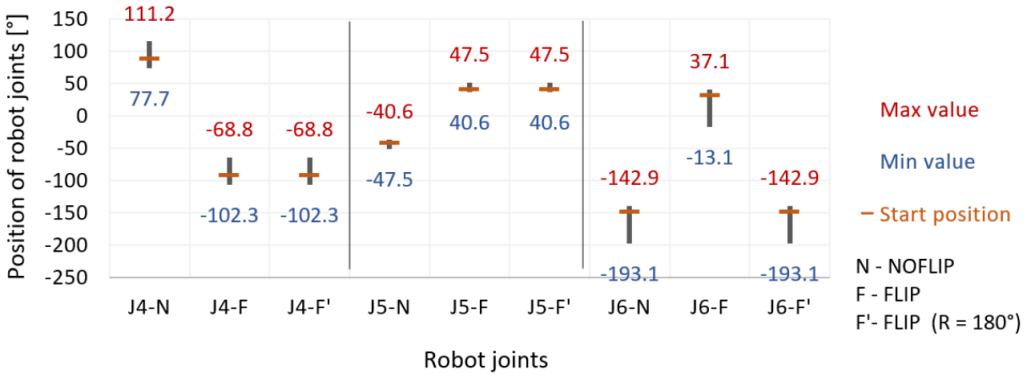

Figure 12. Impact of TCP coordinate modification on the movement of robot joints.

Subsequently, practical measurements were done, with a change applied to individual points of the control program with the adjustment of the coordinate R = 180°. The conditions of this measurement were identical to the conditions from Table 4, with the number of repeated measurements being ten. The resulting polar graph is shown in Figure 13c. In comparison to previous measurements (Figure 13a,b), it is apparent that the change in the motion of the J6 joint does not affect the shape of the polar graph. This fact is also confirmed by the average value of circularity given in Table 6, while the difference of 20.4 µm can be considered negligible. Based on the presented results, it can be argued that the change in the shape of the polar graph is caused by the joint J4 or J5, or a combination thereof.

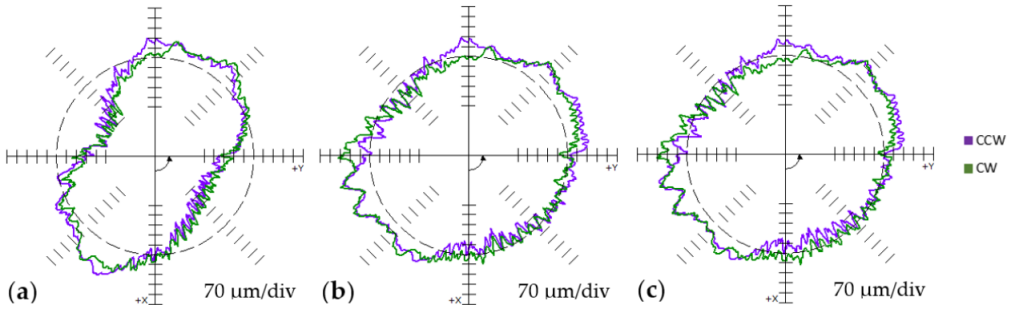

Figure 13. Polar graphs from measuring a circle on the inclined plane. (**a**) NOFLIP configuration; (**b**) FLIP configuration; (**c**) FLIP′ configuration (coordinate R = 180°).

Table 6. Average circularity value for measuring a circle on the inclined plane.

	Configuration NOFLIP	Configuration FLIP	Configuration FLIP′
Circularity [µm]	652.2	409.8	389.3

5.1. Measurement in a Plane Parallel to the Robot's Base

The series of measurements was further supplemented by the measurement of a circular path when the XY plane formed an angle of 0° with the benchtop. The second of the already mentioned jigs was used for this measurement (Figure 7c), which ensured that the central position of the circle was identical to its central position in the previous measurements. Compared to measurements on an inclined plane, the ranges of motions of the individual robot joints are different, with the J4 joint not participating in the movement and its rotation has a constant value throughout the measurement. The absolute values of the range of motion of the individual robot joints measured on an inclined plane (at an angle of −45°) and a plane parallel to the base of the robot (angle 0°) are shown in the graph in Figure 14.

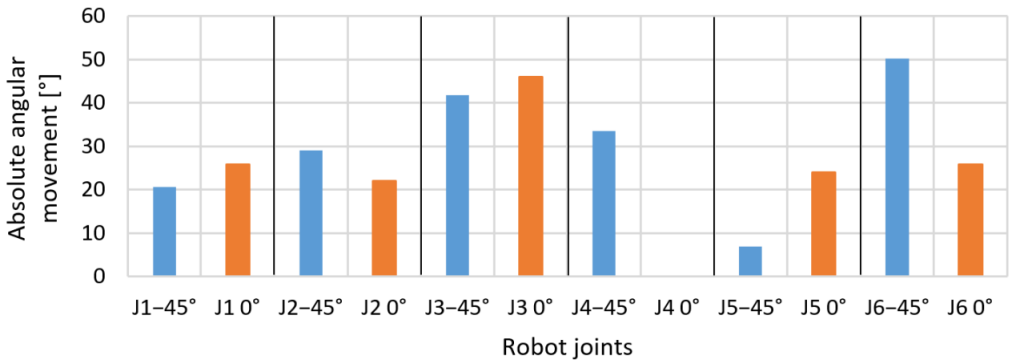

Figure 14. Absolute angular movement of robot joints during the movement along a circular path in both measuring planes.

There are also two possible configurations of the robot arm for the selected position and orientation of the circle. For the configuration with the joint position J5 < 0° (NOFLIP), the J4 joint has a constant value of 0° throughout the path traveled. The circular path can also be completed with the second configuration, i.e., J5 > 0° (FLIP), but in this case, the J4 joint acquires the limit values of its range of rotation, which are +180° or −180°. Such position of the robot arm, with limit values of one of the joints, is unsuitable due to the restriction on further movements, but it can meet the purpose of the measurement. At the same time, to ensure that the range of motion of the J6 joint was the same for all three mentioned positions of the robot arm in the measurement process, the "W" coordinate of individual points forming the circle was again adjusted to 180° in the FLIP configuration. The ranges of motions of the J4, J5, and J6 joints, when moving along the circular path, are shown in the graph in Figure 15. Again, as in the previous cases, positional analysis in the Creo Parametric system 5.0.4.0 was used to chart this graph. For the sake of simplicity, the graph does not include the range of motions of the J1, J2, and J3 joints, which are identical for all positions of the robot arm used.

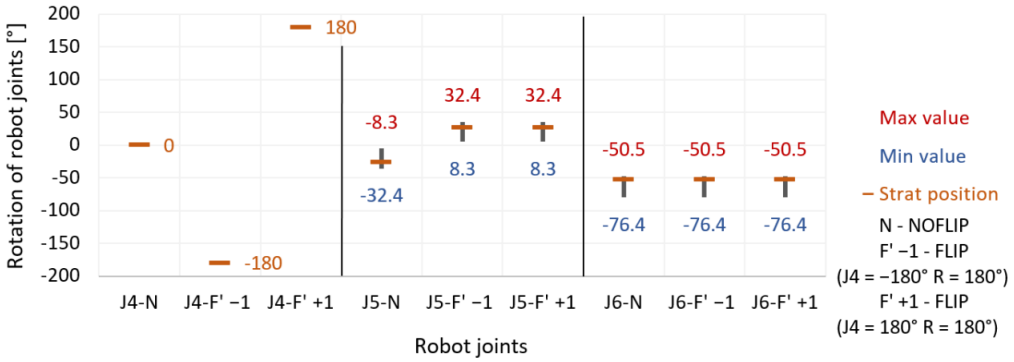

Figure 15. Position of robot joints J4, J5, and J6 when measured in the plane parallel to the base of the robot.

Measurements with the Renishaw Ballbar QC20–W were conducted under the same conditions as in Table 4, except for the orientation of the center of the circular path, which is zero (W = 0°; P = 0°; R = 0°) in the present case. The individual polar graphs are shown in Figure 16 and the average circularity values from ten repeated measurements for each robot arm position used are shown in Table 7.

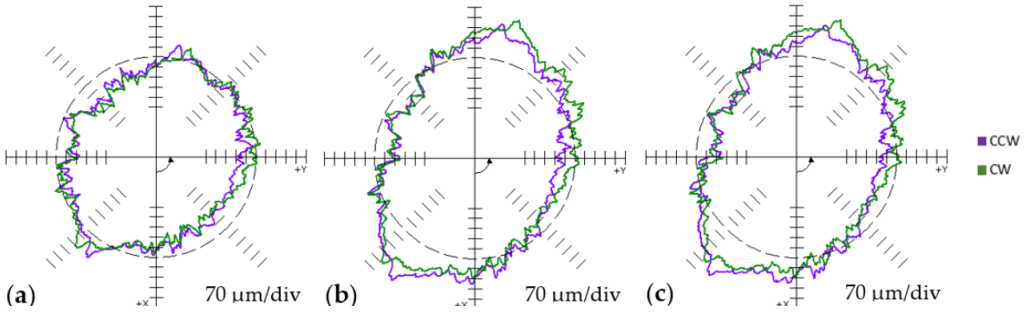

Figure 16. Polar graphs from measuring a circle on the plane parallel to the base of the robot. (**a**) NOFLIP configuration; (**b**) FLIP′ −1 configuration (J4 = −180°, R = 180°); (**c**) FLIP′ +1 configuration (J4 = 180°, R = 180°).

Table 7. Average circularity value for measuring a circle on the plane parallel to the base of the robot.

	Configuration NOFLIP	**Configuration FLIP′ −1**	**Configuration FLIP″ +1**
Circularity [µm]	385.2	508.3	505.6

When comparing the resulting polar graphs, the first thing to be observed is the similarity between the measurements with the FLIP configuration of the arm. The similarity is also indicated by the value of circularity shown in Table 7, the resulting difference is negligible. During both measurements in the FLIP configuration, the motions of all joints were identical except for the J4 joint, which did not take part in the movement along the circular path but acquired a different limit value in both cases. In the case of Figure 16b, the limit value of the J4 joint was −180° and vice versa, when measured as shown in Figure 16c, this limit value was + 180°. Based on these results, it can be said that the static value of the J4 joint rotation does not affect the measurement results. In terms of measurement errors, both graphs reveal the squareness error and the scaling error.

A fundamental influence on the shape of the polar graph and, at the same time, the value of circularity is exerted by a change in the configuration of the robot arm, i.e., the motion of the J5 joint, which can be seen when comparing the polar graph of Figure 16a with the previous two graphs of Figure 16b,c, respectively. At the same time, in this polar graph of the NOFLIP configuration (Figure 16a), it is possible to observe a smaller manifestation of the squareness error than in other measurements. In terms of the shape of the circular path being affected, the relevant changes can be attributed to the motion of the J5 joint.

5.2. Results Summary

As part of measurements with the Renishaw Ballbar QC20–W, the possibility of measuring a circular path placed on an inclined plane has been confirmed as viable. The conducted experiments consisted of two series of measurements. The first of them was done with the circle radius of 100 mm, placed on an inclined plane at an angle P = −45° concerning the robot's WCS. Two possible arm configurations—NOFLIP and FLIP, exist for the selected position and orientation of the measuring plane. The results of the measurements and their representation in polar graphs show a significant difference in the shape of the circular path between the two configurations. This difference has also been confirmed by the average circularity values in both measurements. Based on the motion analysis of the individual robot joints in connection with polar graphs, the motion of the J4, J5, and J6 joints was identified as a possible source of these errors. Subsequent measurements ruled out the effect of the J6 joint. The mentioned measurement was based on the modification of the robot program so that in two measurements in the FLIP configuration, the motion was different only in joints J4 and J5. The motion of the other joints during the measurement was identical.

The second series of measurements took place with the same radius of the circle −100 mm, but in a plane parallel to the base of the robot or parallel to the workbench. These measurements aimed to further examine the influence of the J4 and J5 joints on the measurement results. With the selected orientation of the measuring plane, the position of the joint J4 is static during the entire travel along the circular path. Depending on the selected configuration, the respective values are 0°, −180°, or 180°. By analyzing the range of motion of individual robot joints and the polar graphs obtained from the measurement, the greatest influence on the deformation of the circular path can be attributed to the selected configuration of the robot arm and especially the motion of the J5 joint.

Although both series of measurements took place in two different orientations of the measuring XY plane, the center of the circular path was the same for both orientations. Partial similarity when comparing the polar graphs obtained in the measurement on an inclined plane and the FLIP configuration, with the polar graph in the second series of NOFLIP measurements and configurations, relates to this fact. This similarity is also indicated by the value of circularity, which takes on values of 409.8 µm, or 389.3 µm at an inclined plane, and a value of 385.2 µm when measured in a plane parallel to the robot base. At the same time, when comparing the ranges of motion of the J5 joint, it is possible to rule out their mutual similarity of motion in the above-mentioned configurations and orientations of the circular path. Based on this, it can be argued that the change in the

shape of the polar graph is influenced not only by the J5 joint but also by the motion of the joint J4. When measuring was done in a plane parallel to the robot base, the mentioned influence of the J4 joint was corrected, as the J4 joint acquired only static values.

6. Conclusions

Renishaw Ballbar QC20–W is a tool designed and used specifically for troubleshooting CNC machine tools with a Cartesian kinematic system. When used in connection with industrial robots, it is necessary to proceed from the fact that, unlike CNC machine tools, the circular motion required for measurement is created by the simultaneous motion of several or all of the robot joints. Differences in the kinematics of CNC machine tools and industrial robots renders Ballbar software incapable of identifying and evaluating errors of industrial robots. Therefore it is necessary to approach measurements and evaluation differently. In the case of standard measurement of industrial robots, when the measuring plane is parallel to the robot base, not all robot joints move. The same applies to the so-called volumetric analysis, in which the circle in the XY plane is supplemented by two more circular arcs in the mutually perpendicular planes ZX and ZY. The purpose of the experiments of the present paper was to verify the hypothesis of the motion of all the robot joints when the desired circular path is placed on an inclined plane. The impetus for this work was the measurements previously done with the Renishaw Ballbar at the Department of Automation and Production Systems.

The individual experiments described in the paper can be divided into two parts, preceded by setting the conditions for and preparing the experiment. The key step was the choice of the orientation of the measuring plane in the workspace of the selected Fanuc LR Mate 200iC robot. Based on the recommendations of the ISO 9283 standard, which deals, among other things, with the conditions for measuring the operating characteristics of industrial robots, an inclined plane at an angle of -45° (rotation around the Y–axis) was chosen in the robot's WCS. The starting points for determining other conditions have already been mentioned in experiments conducted in the past.

In the first part of the experiments, a positional analysis was performed with a simulation model of the LR Mate 200iC robot in the environment of the Creo Parametric software 5.0.4.0. The result is the confirmation of the hypothesis that when placing a circle on the selected inclined plane, all its joints, including the J4 joint, would participate in the circular movement of the TCP robot. Commonly, when the measuring plane is parallel to the robot base, the J4 joint is static throughout the movement. The results of the positional analysis were subsequently used to evaluate the results of measurements. The practical measurements with the Renishaw Ballbar QC20–W are described in the second part of this paper. The analysis of the measurement results was performed using polar graphs and circularity values, which represent one of the possible outputs of the Ballbar 20 software. Two series of measurements were done. In the first series, a circle with a radius of 100 mm was placed on an inclined plane, under the before-mentioned angle. The second series represented measurements in a plane parallel to the robot base. In addition to the measurement conditions, the common feature of all measurements was also the identical position of the center of the circle in the robot's workspace. Only the orientation of the measuring plane has changed. The result is the finding that in the selected position and orientation of the measuring plane, the change in the shape of the polar graph was locally caused mainly by a change in the configuration of the robot arm, which is related to the motion of the J4 and J5 joints. At the same time, the similarity of the results was observed when comparing the two series of measurements, which can be attributed to the just mentioned unchanged position of the center of the circular path.

The measurement on an inclined plane provides mainly a better view of industrial robot properties. The standard measurement of industrial robot properties that utilize the Renishaw Ballbar system is conducted on the plane parallel to its base plane. We used such a measurement method in previous works [25,26,28]. However, the parallel orientation of the measuring plane results in the uneven involvement of individual motors on the

overall motion of the TCP. In particular, the joint J4 is static throughout the whole path both for measuring in the parallel plane and for volumetric measurement too. The pro-posed method places the measuring path on an inclined plane, which results in movement that involves all of the robot joints, including J4. The results of such measurements offer better information about the technical condition of the robot including the possible impact of the J4 joint. The presented measurement method can be used in process of industrial robot condition monitoring based on measurements repeated in regular intervals. The changes can be evaluated by changes in the shape of the polar chart. It is important to include all of the possible unwanted effects that can affect the performance of the industrial robot.

Possible Further Work

The LR Mate 200iC robot used had been calibrated several times in the past, with the application of the so-called Zero position master method. The accuracy of this method is based only on the visual adjustment of the individual joints of the robot to the zero position, using reference marks. Therefore, this calibration method is considered inaccurate, that fact is also pointed out in the Fanuc robot's user manual [40]. The manual emphasizes that the method should only be used in exceptional cases. Such a state of affairs was addressed in the past by refining the calibration, using original calibration data. In connection with the identified influence of the motion of the J4 and J5 joints on the final shape of the polar graph and the overall measurement results, it is possible to look for the cause probably in the still persistent inaccurate calibration of the given robot. Based on this, there is room for further work and repetition of the measurements presented, subject to a more detailed specification of the LR Mate 200iC robot calibration. There is also room for comparison with a robot of a clearly more accurate calibration than that of the robot used in the experiments described in our paper.

It is possible to use Renishaw Ballbar to evaluate individual properties of industrial robots defined in ISO 9283 standard. The double ballbar measuring technique is based on periodical measuring of deviation of the real radius from programmed one during the movement in a circular path. It is possible to utilize such a measurement technique for the evaluation of so-called path accuracy (AT according to ISO 9283) and path repeatability (RT according to ISO 9283). Path accuracy characterizes the ability of a robot to move its mechanical interface along the command path in the same direction n times [6]. Path repeatability expresses the closeness of the agreement between the attained paths for the same command path repeated n times [6]. Measured values are important for the calculation of both mentioned properties. A good example is a measurement on the inclined plane using NOFLIP configuration, measurement conditions are included in Table 4 and the polar graph is shown in Figure 10a. In this case, the average radius of ten repeated measurements (clockwise) was between 99.594 mm and 100.201 mm. In order to reliably determine the values of RT and AT, it is necessary to analyze measurement records more and to define the correct methodology of evaluation. The measurements collected with Ballbar 20 software can be too distorted for this purpose, as the software subtracts estimated eccentricity represented by the first harmonics of the measured profile processed by fast Fourier transformation. For evaluation and calculation of the performance parameters of the industrial robot, it would be necessary to get values declared by its manufacturer as they usually declare only unidirectional path repeatability (RP according to ISO 9283). Another possible way to verify results would be to compare it to measurement using a laser interferometer or a laser tracker.

Author Contributions: Conceptualization, Methodology: all authors; Writing—original draft: V.T. and I.Z.; Writing—review and editing: M.C., I.K. and M.S. All authors have read and agreed to the published version of the manuscript.

Funding: This work was supported by the Slovak Research and Development Agency under the contract No. APVV–16–0283.

Institutional Review Board Statement: Not applicable.

Informed Consent Statement: Not applicable.

Data Availability Statement: The data presented in this study are available on request from the corresponding author.

Conflicts of Interest: The authors declare no conflict of interest.

References

1. Heer, C. Top Trends Robotics 2020 (Press Release). Available online: https://ifr.org/ifr-press-releases/news/top-trends-robotics-2020 (accessed on 22 November 2020).
2. Akatov, N.; Mingaleva, Z.; Klackova, I.; Galieva, G.; Shaidurova, N. Expert Technology for Risk Management in the Implementation of QRM in a High-Tech Industrial Enterprise. *Manag. Syst. Prod. Eng.* **2019**, *27*, 250–254. [CrossRef]
3. Hu, M.; Wang, H.; Pan, X.; Tian, Y. Optimal Synthesis of Pose Repeatability for Collaborative Robots Based on the ISO 9283 Standard. *Ind. Robot Int. J. Robot. Res. Appl.* **2019**, *46*, 812–818. [CrossRef]
4. Bulej, V.; Stanček, J.; Kuric, I.; Zajacko, I. The Space Distribution and Transfer of Positioning Errors from Actuators to the TCP Point of Parallel Mechanism. In Proceedings of the MATEC Web of Conferences, Sklene Teplice, Slovakia, 5–8 September 2017; Volume 157.
5. Slamani, M.; Nubiola, A.; Bonev, I.A. Modeling and Assessment of the Backlash Error of an Industrial Robot. *Robotica* **2012**, *30*, 1167–1175. [CrossRef]
6. *ISO 9283:1998 Manipulating Industrial Robots—Performance Criteria and Related Test Methods*; International Organization for Standardization: Geneva, Switzerland, 1998.
7. *ISO/TR 13309:1995 Manipulating Industrial Robots—Informative Guide on Test Equipment and Metrology Methods of Operation for Robot Performance Evaluation in Accordance with ISO 9283*; International Organization for Standardization: Geneva, Switzerland, 1995.
8. Dandash, D.; Brethe, J.-F.; Vasselin, E.; Lefebvre, D. Micrometre Scale Performances of Industrial Robot Manipulators. *Int. J. Adv. Robot. Syst.* **2012**, *9*. [CrossRef]
9. Brethé, J.-F.; Lefebvre, D. Risk Ellipsoids and Granularity Ratio for Industrial Robots. *Int. J. Fact. Autom. Robot. Soft Comput.* **2007**, *2*, 93–101.
10. Şirinterlikçi, A.; Murat, T.; Bird, A.; Harris, A.; Kweder, K. Repeatability and Accuracy of an Industrial Robot: Laboratory Experience for a Design of Experiments Course. *Technol. Interface J.* **2009**, *9*, 1–10.
11. Pastor, M.; Zivcak, J.; Puskar, M.; Lengvarsky, P.; Klackova, I. Application of Advanced Measuring Methods for Identification of Stresses and Deformations of Automotive Structures. *Appl. Sci.* **2020**, *10*, 7510. [CrossRef]
12. Jiang, Y.; Yu, L.; Jia, H.; Zhao, H.; Xia, H. Absolute Positioning Accuracy Improvement in an Industrial Robot. *Sensors* **2020**, *20*, 4354. [CrossRef] [PubMed]
13. Icli, C.; Stepanenko, O.; Bonev, I. New Method and Portable Measurement Device for the Calibration of Industrial Robots. *Sensors* **2020**, *20*, 5919. [CrossRef]
14. Nubiola, A.; Bonev, I.A. Absolute Calibration of an ABB IRB 1600 Robot Using a Laser Tracker. *Robot. Comput. Integr. Manuf.* **2013**, *29*, 236–245. [CrossRef]
15. Jozwik, J.; Ostrowski, D.; Jarosz, P.; Mika, D. Industrial Robot Repeatability Testing with High Speed Camera Phantom V2511. *Adv. Sci. Technol. Res. J.* **2016**, *10*, 86–93. [CrossRef]
16. Abderrahim, M.; Khamis, A.; Garrido, S.; Moreno, L. Accuracy and calibration issues of industrial manipulators. In *Industrial Robotics: Programming, Simulation and Application*; I-Tech: Madrid, Spain, 2004; pp. 131–146.
17. Goetz, C.; Tuttas, S.; Hoegner, L.; Eder, K.; Stilla, U. Accuracy Evaluation for a Precise Indoor Multi-Camera Pose Estimation System. In Proceedings of the PIA11: Photogrammetric Image Analysis, Munich, Germany, 5–7 October 2011; Stilla, U., Rottensteiner, F., Mayer, H., Jutzi, B., Butenuth, M., Eds.; Copernicus Gesellschaft Mbh: Gottingen, Germany, 2011; Volume 38–3, pp. 97–102.
18. Jozwik, J.; Jacniacka, E.; Ostrowski, D. Estimation of Uncertainty of Laser Interferometer Measurement in Industrial Robot Accuracy Tests. In Proceedings of the II International Conference of Computational Methods in Engineering Science (CMES'17), Lublin, Poland, 23–25 November 2017; Borys, M., Czyz, Z., Falkowicz, K., Kujawska, J., Kulisz, M., Szala, M., Eds.; EDP Sciences: Les Ulis, France, 2017; Volume 15.
19. Slamani, M.; Joubair, A.; Bonev, I.A. A Comparative Evaluation of Three Industrial Robots Using Three Reference Measuring Techniques. *Ind. Robot. Int. J. Robot. Res. Appl.* **2015**, *42*, 572–585. [CrossRef]
20. Slamani, M.; Bonev, I.A. Characterization and Experimental Evaluation of Gear Transmission Errors in an Industrial Robot. *Ind. Robot. Int. J. Robot. Res. Appl.* **2013**, *40*, 441–449. [CrossRef]
21. Jozwik, J.; Kuric, I.; Ostrowski, D.; Dziedzic, K. Industrial Robot Accuracy Testing with QC20-W Ballbar Diagnostic System. *Manuf. Technol.* **2016**, *16*, 519–524. [CrossRef]
22. Slamani, M.; Nubiola, A.; Bonev, I. Assessment of the Positioning Performance of an Industrial Robot. *Ind. Robot. Int. J. Robot. Res. Appl.* **2012**, *39*, 57–68. [CrossRef]
23. Nubiola, A.; Slamani, M.; Bonev, I.A. A New Method for Measuring a Large Set of Poses with a Single Telescoping Ballbar. *Precis. Eng.* **2013**, *37*, 451–460. [CrossRef]

24. Cubonova, N.; Dodok, T.; Sagova, Z. Optimisation of the Machining Process Using Genetic Algorithm. *Sci. J. Silesian Univ. Technol. Ser. Transp.* **2019**, *104*, 15–25. [CrossRef]
25. Kuric, I.; Tlach, V.; Cisar, M.; Sagova, Z.; ZajaCko, I. Examination of Industrial Robot Performance Parameters Utilizing Machine Tool Diagnostic Methods. *Int. J. Adv. Robot. Syst.* **2020**, *17*. [CrossRef]
26. Tlach, V.; Ságová, Z.; Kuric, I. Circular and Quasi-Circular Paths for the Industrial Robots Measuring with the Renishaw Ballbar QC20-W. In Proceedings of the MATEC Web of Conferences, Rydzyna, Poland, 4–7 September 2018; Volume 254, p. 5007.
27. Kuric, I.; Císar, M.; Tlach, V.; Zajačko, I.; Gál, T.; Więcek, D. *Technical Diagnostics at the Department of Automation and Production Systems*; Springer: Cham, Switzerland, 2019; Volume 835, ISBN 9783319974897.
28. Tlach, V.; Císar, M.; Kuric, I.; Zajačko, I. Determination of the Industrial Robot Positioning Performance. In Proceedings of the MATEC Web of Conferences, Cluj Napoca, Romania, 12–13 October 2017; Balc, N., Ed.; EDP Sciences: Les Ulis, France, 2017; Volume 137, p. 1004.
29. Renishaw PLC. *QC20-W Wireless Ballbar System Description and Specifications*; Renishaw PLC: Wotton-under-Edge, UK, 2013.
30. Dodok, T.; Čuboňová, N. Application of strategy manager tools for optimized NC programming. In *Lecture Notes in Mechanical Engineering*; Springer International Publishing AG: Cham, Switzerland, 2019; pp. 322–334.
31. *ISO 230-4:2005 Test Code for Machine Tools—Part 4: Circular Tests for Numerically Controlled Machine Tools*; International Organization for Standardization: Geneva, Switzerland, 2005.
32. Cunningham, J.; Xu, Q.; Ford, D.G. A Case Study on Practical Error Correction Practices Utilized on a CNC Machine Tool. In Proceedings of the 18th National Conference on Manufacturing Research, Leeds, UK, 10–12 September 2002; pp. 361–366.
33. Yang, S.-H.; Lee, H.-H.; Lee, K.-I. Identification of Inherent Position-Independent Geometric Errors for Three-Axis Machine Tools Using a Double Ballbar with an Extension Fixture. *Int. J. Adv. Manuf. Technol.* **2019**, *102*, 2967–2976. [CrossRef]
34. Poppeova, V.; Bulej, V.; Zahoransky, R.; Uricek, J. Parallel Mechanism and Its Application in Design of Machine Tool with Numerical Control. In Proceedings of the Robotics in Theory and Practice, Strbske Pleso, Slovakia, 14–16 November 2013; Pachnikova, L., Hanjuk, M., Eds.; Trans Tech Publications Ltd.: Durnten-Zurich, Switzerland, 2013; Volume 282, pp. 74–79.
35. *FANUC Robotics SYSTEM R-30iA HandlingTool Setup and Operations Manual. MAROC77HT01101E REV B*; FANUC America Corporation: Michigan, MI, USA, 2015.
36. PTC To Define a Motor. Available online: http://support.ptc.com/help/creo/creo_pma/usascii/index.html#page/simulate%2Fdes_anim%2Fservomotors%2Fto_create_servo.html%23wwconnect_header (accessed on 2 December 2020).
37. Kwon, Y.; Ertekin, Y.M.; Tseng, B. In-Process and Post-Process Quantification of Machining Accuracy in Circular CNC Milling. *Mach. Sci. Technol.* **2005**, *9*, 27–38. [CrossRef]
38. Kuric, I.; Císar, M. Machine Tool Errors and Its Simulation on Experimental Device. *Acad. J. Manuf. Eng.* **2015**, *13*, 17–21.
39. Karan, B.; Vukobratovic, M. Calibration and Accuracy of Manipulation Robot Models—An Overview. *Mech. Mach. Theory* **1994**, *29*, 479–500. [CrossRef]
40. *FANUC Robot LR Mate 200iC. Maintenance Manual. B-82585EN/04*; FANUC America Corporation: Michigan, MI, USA, 2008.